PHYSICAL REVIEW B **83**, 115203 (2011)

Enhanced Curie temperature and nonvolatile switching of ferromagnetism in ultrathin (Ga,Mn)As channels

I. Stolichnov,[1] S. W. E. Riester,[1] E. Mikheev,[1] N. Setter,[1] A. W. Rushforth,[2] K. W. Edmonds,[2] R. P. Campion,[2] C. T. Foxon,[2] B. L. Gallagher,[2] T. Jungwirth,[3,2] and H. J. Trodahl[4]

[1]*Ceramics Laboratory, EPFL-Swiss Federal Institute of Technology, Lausanne 1015, Switzerland*
[2]*School of Physics and Astronomy, University of Nottingham, Nottingham NG7 2RD, United Kingdom*
[3]*Institute of Physics ASCR v.v.i., Cukrovarnická 10, CZ-162 53 Praha 6, Czech Republic*
[4]*MacDiarmid Institute for Advanced Materials and Nanotechnology, Victoria University, Wellington, New Zealand*

(Received 5 January 2011; published 16 March 2011)

The integration of ferroelectric polymer gates on a Mn-doped GaAs magnetic channel provides a promising route for the persistent field-effect control of magnetic properties in high-quality diluted magnetic semiconductors (DMSs) that are otherwise incompatible with traditional oxide ferroelectrics. That control demands the thinnest possible DMS layers, for which to date the Curie temperature (T_C) is severely depressed. Here we show that reducing the channel thickness from 7 to 3–4 nm by etching, followed by a brief 135 °C anneal, does not degrade the T_C ($\sim$70 K) of the 7-nm film. The channel thinning results in a dramatic threefold increase of the T_C shift controlled by the ferroelectric polarization reversal. Furthermore, we obtain the same exponent $(\partial \ln T_C/\partial \ln R) \equiv \gamma \approx -0.3$ for all channels with different thicknesses, regardless of the technique used for T_C determination. These results suggest that the ferromagnetic coupling in an ultrathin 3-nm channel is far from the two-dimensional limit and shows a rather bulklike behavior, similar to well-established 7-nm films.

DOI: 10.1103/PhysRevB.83.115203 PACS number(s): 85.75.−d, 77.84.Jd, 85.30.Tv, 75.50.Pp

I. INTRODUCTION

Magnetoelectric multiferroics, systems showing coupled ferroelectricity and ferromagnetism, have emerged within the past decade as a very active field of research, driven by their potential for electronic and spintronic exploitation.[1] Although there is a focus on single-phase multiferroics,[2] the stronger multiferroic coupling that is possible in composite multiferroics makes these systems attractive for many potential applications (e.g., spintronic logic and memory elements).[3] A great deal of early work concentrated on structures in which the coupling was mediated by electro- and magnetostriction effects,[4] but more recently structures relying on electric-field-mediated multiferroic coupling have been demonstrated.[5,6] In addition to the potential for enhanced coupling, these structures show a way toward field-effect devices compatible with complementary metal-oxide semiconductor (CMOS) circuitry.

A field-mediated multiferroic device requires intimate contact between a ferroelectric gate and a ferromagnetic material, such as a diluted magnetic semiconductor (DMS), in which a carrier-mediated exchange interaction permits the carrier-density modulation of the magnetic response. However, the practical realization has been limited by the need to ensure processing compatibility between the ferroelectric and ferromagnetic components. In particular, perovskite ferroelectrics require high-temperature processing that is detrimental to the common (III,Mn)V ferromagnetic semiconductors that can be directly integrated with semiconductor electronic or spintronic devices. As a consequence, lanthanum manganites such as $La_xSr_{1-x}MnO_3$ (LSMO), which are stable at high temperatures, have been considered as the primary candidates for the ferromagnetic element in the composite multiferroic systems. They offer epitaxial-growth compatibility with $Pb(Zr_x,Ti_{1-x})O_3$ (PZT) and other perovskites, and their magnetic properties are sensitive to the carrier concentration. A change of magnetic properties associated with the polarization state in the ferroelectric layer has been confirmed in LSMO via the magnetoresistance measurements[7] and more recently by analysis of tunnel-current spin polarization[8] and magneto-optic Kerr effect magnetometry.[6] In the latter case a significant Curie temperature (T_C) shift of 18 K has been reported in the ultrathin LSMO layer with integrated epitaxial PZT gate. However, this approach still suffers from a processing incompatibility with semiconductor circuitry.

An alternative approach to realize the composite multiferroic system is based on a well-established diluted magnetic semiconductor (Ga,Mn)As.[5,9] We have previously shown that the compatibility problem can be resolved by using a ferroelectric copolymer of polyvinylidene fluoride with trifluoroethylene, P(VDF-TrFE). The ferroelectric control of ferromagnetism in this system was successfully demonstrated by measuring changes of T_C and hysteretic properties between the accumulation and depletion states. A modest persistent T_C shift of 3–4 K was observed in previous experiments, and in this paper we report a threefold enhancement in carefully annealed ultrathin films.

The level of persistent accumulation and/or depletion induced by a ferroelectric gate is limited to its spontaneous polarization, 7–8 $\mu C/cm^2$ for PVDF, and by screening at the semiconductor interface. The modulation is further reduced by the weak dependence of the Curie temperature on the carrier density, $T_C(p) \sim p^{1/3}$, that is expected for (Ga,Mn)As within the Zener mean-field model.[10] It was recently shown by modeling and confirmed experimentally using normal (nonferroelectric) gates that for 4–7 nm (Ga,Mn)As channels with strongly nonuniform depletion profiles the dependence of T_C on hole sheet concentration p_s obeys an even weaker power law $T_C \sim p_s^{0.2}$.[11] The strongest ($\Delta T_C = 17$ K) *nonpersistent* field-effect control of the ferromagnetism in a (Ga,Mn)As channel has been demonstrated using 3.5 nm films and a high-ε dielectric HfO_2 gate.[12] However, the magnetic properties of the

 ©2011 American Physical Society

ultrathin channel were severely degraded with T_C close to 30 K, substantially lower when compared to the Curie temperature of ∼70–80 K typical for moderately annealed 7-nm films with the same composition.

Clearly it is desirable to explore T_C modulation in the polymer ferroelectric gated configuration with the thinnest possible layers and the largest T_C in order to optimize the exploitable action of a PVDF gate. Here we report successful experiments along this research path, based on a gradual thinning of the (Ga,Mn)As magnetic channel by postgrowth etching. To prevent degradation of ferromagnetic properties after etching we perform careful low-temperature annealing of the channel. The low-temperature annealing is known to remove interstitial Mn impurities that are detrimental to ferromagnetism because they act as charge and moment compensating defects.[10] We will show that a strongly reduced T_C after etching can be almost fully recovered by annealing, but with the sheet hole concentration reduced in the thinned channel. The etching and annealing process thus offers an opportunity to enhance the electric field-effect control of ferromagnetism without significant degradation of the ferromagnetic moment or Curie temperature of the channel.

II. EXPERIMENTAL DETAILS

7-nm (Ga,Mn)As layers with 6% nominal Mn doping used in this study were grown by low-temperature molecular-beam epitaxy as described earlier.[5] Standard Hall bars were defined by photolithography and chemical etching, and Ti/Au (15/100 nm) contacts were deposited by electron-beam evaporation and patterned by the lift-off technique. To change the (Ga,Mn)As channel thickness we etched the Hall bars in 10% HCl, which removes the surface oxide.[13] After the oxide removal the sample was left at ambient conditions for 6 h to form the new native oxide layer on the surface. Variable channel thicknesses in Hall bars cleaved from the same wafer were prepared by repeating the etching step up to six times. A ferroelectric gate comprising a 250-nm layer of a P(VDF-TrFE) ferroelectric polymer was spin coated on the Hall bars from a 2.5% solution of methyl ethyl ketone and then annealed at 136 °C for 15 min. 100-nm gold gate electrodes were thermally evaporated. The gate was poled by applying a negative (positive) bias of 14 V in order to induce accumulation (depletion) in the ferromagnetic channel. The magnetic properties of the Hall bar devices were evaluated by measuring T_C using two techniques based on conductivity and magnetotransport measurements. The first technique determines T_C from the position of the cusp of the derivative of the temperature-dependent zero-field resistance, $\partial R/\partial T$.[14] The second relies on a conventional Arrott-plot analysis, using the extraordinary Hall effect to represent the magnetization in the film. In this technique, T_C is the temperature at which the intercept of the Arrott plot at zero field passes through zero.[15] The former method is clearly the more reliable measure of the zero-field ferromagnetic ordering temperature, and it shows a sharp cusp at a well-defined temperature in all studied samples. We have not used another common signature based on the peak of the resistance, which overestimates both T_C and its modulation between the accumulation and depletion states.[5]

III. RESULTS AND DISCUSSION

In addition to the three samples with different magnetic channel thicknesses used for the ferroelectric gate experiment, supplementary Hall bars were fabricated in order to investigate conductivity versus the number of etching steps and to evaluate

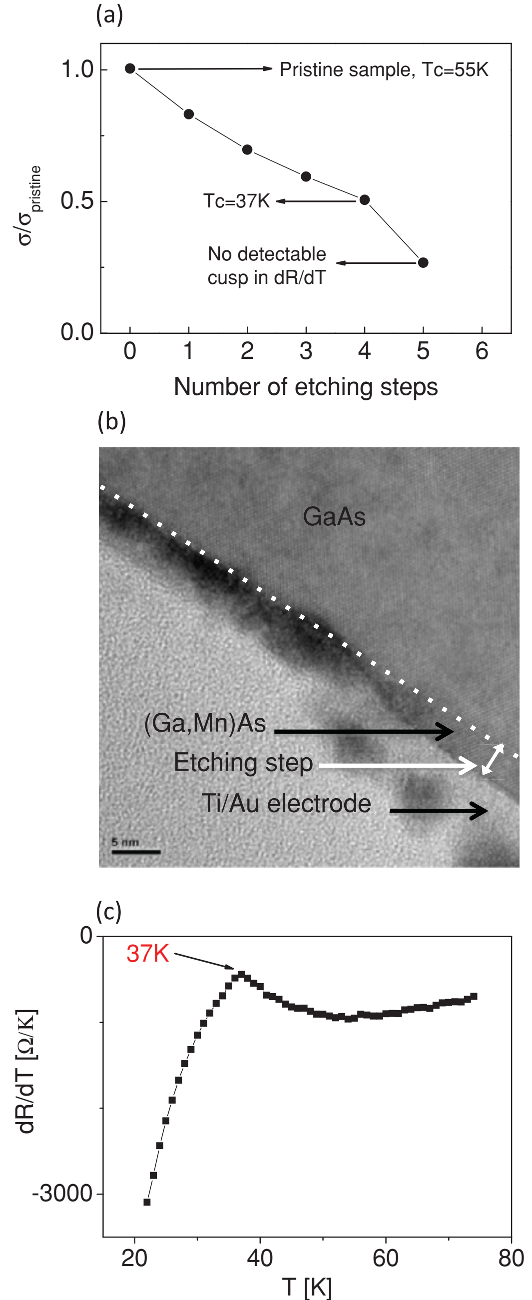

FIG. 1. (Color online) Change of the (Ga,Mn)As magnetic channel thickness by chemical etching. (a) Normalized room-temperature conductivity measured on the reference Hall bar after etching and reoxidizing as a function of number of etching steps. (b) TEM cross-section image of the (Ga,Mn)As channel taken after four consecutive etching runs. The image is taken at the border of the electrode in order to visualize the step between the part protected by electrode and the etched area. (c) Temperature derivative of the measured resistivity for the channel with thickness reduced to <3.5 nm. T_C signaled by cusp of the resistance derivative is 37 K.

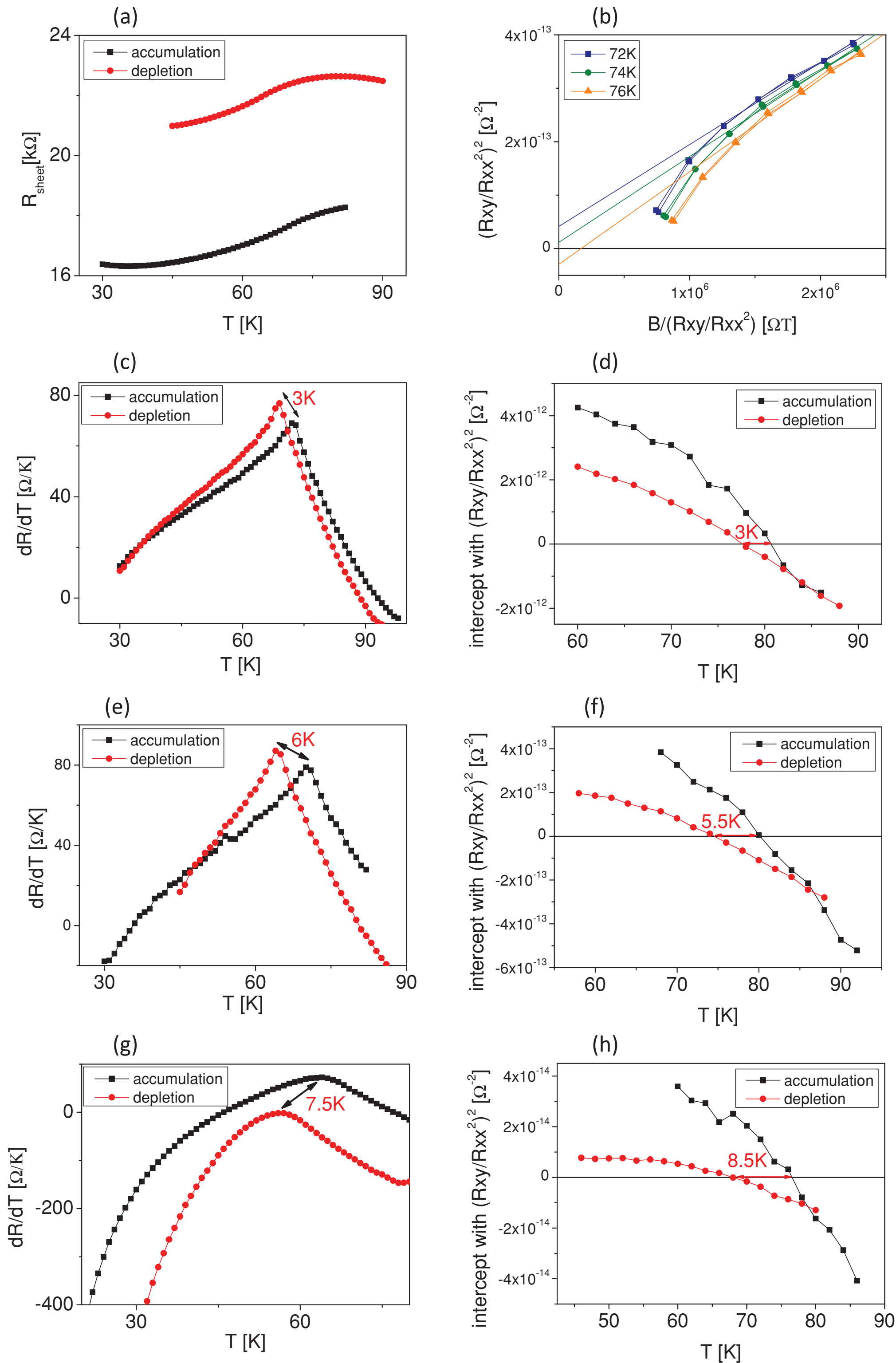

FIG. 2. (Color online) Persistent gate effect on the (Ga,Mn)As magnetic channel resistance and T_C. (a) Temperature-dependent sheet resistance of the channel in the depletion and accumulation poled states. (b) Example of Arrott plots for the moderately etched sample (II). (c) and (d) Sample I: Determination of T_C in the accumulation and depletion states using the cusp of the resistance derivative (c) and intercepts of Arrott graphs plotted vs temperature (d). (e) and (f) Same analysis for sample II. (g) and (h) Same analysis for sample III.

the magnetic properties prior to the gate deposition. Figure 1(a) shows the normalized room-temperature conductivity measured on these Hall bars after etching and reoxidizing, showing a nearly linear decrease with the number of etching steps. In order to evaluate directly the etching speed, we have performed a transmission electron microscopy (TEM) analysis of the

TABLE I. Sheet resistance, T_C, and exponent $\gamma = \partial(\ln T_C)/\partial(\ln R)$ in the accumulation (Acc.) and depletion (Dpl.) states. T_C's have been extracted from the Arrott plots (upper part) and alternatively from the $\partial R/\partial T$ cusp (lower part).

	R_s at T_C, Acc. (Ω)	R_s at T_C, Dpl. (Ω)	T_C, Acc. (K)	T_C, Dpl. (K)	$\partial(\ln T_C)/\partial(\ln R)$
		T_C extracted from the Arrott plots			
I	12.22	13.82	81	78	−0.31
II	18.21	22.55	80	74.5	−0.33
III	33.04	48.87	76.5	68	−0.30
		T_C extracted from the $\partial R/\partial T$ cusp			
	R_s at T_C, Acc. (Ω)	R_s at T_C, Dpl. (Ω)	T_C, Acc. (K)	T_C, Dpl. (K)	$\partial(\ln T_C)/\partial(\ln R)$
I	11.75	13.22	72	69	−0.36
II	17.65	21.95	70	64	−0.41
III	32.53	49.30	64	56.5	−0.30

etched Hall bar cross section. The TEM image in Fig. 1(b) has been taken after four consecutive etching runs at the border of the electrode in order to determine the step between the part of the channel protected by the electrode and the etched area. The TEM image indicates that $\sim$3.5 ± 0.5 nm (Ga,Mn)As layer has been removed after four etching steps, corresponding to the etching rate of 0.75–1 nm/step. This rate is higher than has been reported previously[13] and can change depending on the sample and etching solution. Thus we adopt as a gauge of the channel thickness the room-temperature conductance measured on the etched Hall bar after the reoxidization rather than the number of etching steps. Assuming a linear change of sheet conductivity with the thickness, we estimate the thickness of the three gated samples presented in this study to be 7 nm (sample I, nonetched), 4.7 nm (sample II, moderately etched), and 3 nm (sample III, heavily etched).

Etched Hall bar devices without ferroelectric gates showed rather low T_C specifically it was only 37 K for the sample with a thickness of 3.5 nm as confirmed by the $\partial R/\partial T$ cusp [Fig. 1(c)]. However, after the deposition of the ferroelectric gate and its annealing at 136 °C for 15 min, the T_C for all three samples increased to 70–80 K and showed only a very weak dependence on the channel thickness. Note that this dramatic increase of T_C has been achieved by a very fast annealing at an extremely low temperature of 136 °C, which is significantly lower than the routinely used 180–200 °C. Thus, far from being detrimental to these very thin DMS layers, the processing of the polymer gate *enhances* their magnetic properties.

We turn now to the results on samples after depositing and poling the PVDF gate (Fig. 2). Examples of the temperature dependence of resistance [Fig. 2(a)] and Arrott plots [Fig. 2(b)] for sample II attest to low-noise magnetotransport data suitable for an accurate analysis of T_C with a precision close to 1 K. Figures 2(c) and 2(d) show, respectively, the sheet resistivity derivative and the Arrott-plot intercept of the thickest nonetched film for both PVDF poling states, all plotted versus the temperature. Figures 2(e) and 2(f) present the same data for the moderately etched sample II while Figs. 2(g) and 2(h) show data for heavily etched sample III. The gate effect was reversible and reproducible; multiple reversals between the accumulation and depletion states yielded identical results.

Table I summarizes the main results of Fig. 2. The data show only a weak suppression of the mean T_C in the thinner films; as mentioned above, all three films exhibit a recovery of T_C after annealing. The annealing-driven recovery results from an increase of the hole concentration p and an increase of concentration of ferromagnetically coupled ions as antiferromagnetically coupled interstitial Mn ions diffuse to the surface. The thermal budget was the same for all three samples, so we interpret the fact that more heavily etched films show a more pronounced T_C recovery is that the diffusion is enhanced in thinner films.[16] It is important to note that the etched films (II and III) reach nearly the same T_C as the unetched reference film (I) while the sheet [two-dimensional (2D)] hole concentration and conductivity of films (II and III) remain smaller.

Despite the 10-K disagreement between the absolute Curie temperatures estimated by Arrott plots and the $\partial R/\partial T$ cusp, the persistent T_C shifts (ΔT_C) show excellent agreement between the two techniques. The magnitude of the Curie temperature change that is induced by the ferroelectric gate increases significantly for the thinner structures, as expected for the stronger modulation of their smaller sheet concentration of exchange-mediating holes. Thus, compared to the reference unetched sample, which shows a relatively modest $\Delta T_C =$ 3 K, the Arrott plots deliver nearly a twofold increase (5.5 K) for sample II and a threefold increase (8.5 K) for sample III. The $\partial R/\partial T$ cusp yields similar ΔT_C enhancements. It is important that this enhancement is accomplished without a pronounced degradation of the mean T_C.

The final columns in Table I show an exponent $(\partial \ln T_C/\partial \ln R) \sim -0.3$ for the three films, somewhat smaller than the result $(\partial \ln T_C/\partial \ln R) \sim -0.5$ we found in an earlier study of a 7-nm film.[5] Furthermore, assuming a linear relationship between the conductivity and hole concentration, one arrives at $T_C \sim p_s^{0.3}$ in these films, in agreement with the predictions of the Zener mean-field model[10] but not with the exponent 0.2 recently reported for the ultrathin films.[11] These

differences are not related to the film thicknesses; note that the present data correspond to thicknesses covering the range of 3–7 nm. Further studies are required to identify the source of the variable responses ($\partial \ln T_C/\partial \ln R$) upon modulating the hole density in very thin (Ga,Mn)As channels observed in different experiments.

The discussion above treats the very thin films as bulklike in their magnetic and conducting properties, despite that there are two relevant scale lengths of order 1 nm: the Thomas-Fermi screening length and the average Mn-Mn separation. The former implies a depth-dependent hole concentration through the channel, which has been modeled previously with a Poisson solver and a hole density of states appropriate for these heavily doped materials. The effect of this inhomogeneous hole distribution has been discussed in detail in relation to a conventional field-effect transistor (FET) control of the hole concentration in similar films.[11] The results demonstrated that it is appropriate to accept the depth-averaged concentration while retaining the bulklike dependence of T_C on p.

The approach of 2D exchange as the film thicknesses become comparable to the Mn-Mn separation is less easily argued. As a guide, note that the exchange coupling that exists among the random sites occupied by Mn ions in (Ga,Mn)As can be modeled as a percolation process.[17] As one approaches the 2D limit, the population fraction of Mn ions that are included in a sample-spanning volume falls; full percolation is less easily achieved in 2D than in 3D. The similar Curie temperatures of the three films of very different thicknesses suggests that at least the major part of the Mn ions align in a sample-spanning ferromagnetic cluster, much as they do in fully 3D films, even at a thickness of (3 nm) only three times the average Mn-Mn separation. A further argument supporting the 3D-like behavior of the etched 3-nm channel is nearly the same value of the exponent γ obtained for all samples from 7 to 3 nm, regardless of the technique of T_C determination. Note, however, that the cusp in the resistance derivative is less sharp in the thinnest film, a phase-boundary broadening that suggests the presence of a fraction of finite exchange-coupled clusters that are at best only weakly coupled to the sample-spanning cluster.

IV. CONCLUSIONS

In conclusion, gradual thinning of (Ga,Mn)As films via the top oxide etching proves to be an efficient approach for enhancement of field-effect-mediated multiferroic coupling. In particular, a nearly threefold increase of a persistent T_C shift has been reached by reducing the channel thickness from 7 to 3 nm. It is particularly significant that the mild annealing required by the polymer gate recovers the Curie temperature measured in the prethinned 7-nm film, thus demonstrating that the loss of exchange strength in ultrathin films is not inevitable. Furthermore, the T_C response to the resistance change driven by the ferroelectric gate switching is characterized by the same exponent $\gamma \approx 0.3$ for all samples with thicknesses ranging from 3 to 7 nm, suggesting that the ferromagnetic coupling in the thinnest 3-nm layer follows the same 3D behavior as the standard 7-nm material. From the technological prospective a dramatic increase of T_C achieved by annealing the magnetic channel at a very low temperature of 136 °C for 15 min, further enhances the compatibility of this multiferroic structure with thermal-budget-sensitive systems.

ACKNOWLEDGMENTS

We acknowledge support from the Swiss National Science Foundation, the EU 7th Framework project NAMASTE-214499, and Czech Republic Grants No. AV0Z10100521, No. LC510, and Preamium Academiae. The authors are grateful to Dr. C. Sandu for the TEM analysis.

[1] W. Eerenstein, N. D. Mathur, and J. F. Scott, Nature (London) **442**, 759 (2006).
[2] N. A. Spaldin and R. Ramesh, MRS Bull. **33**, 1047 (2008).
[3] C. A. F. Vaz, J. Hoffman, C. H. Ahn, and R. Ramesh, Adv. Mater. (Weinheim, Ger.) **22**, 2900 (2009).
[4] W. Eerenstein, M. Wiora, J. L. Prieto, J. F. Scott, and N. D. Mathur, Nat. Mater. **6**, 348 (2007).
[5] I. Stolichnov, S. W. E. Riester, H. J. Trodahl, N. Setter, A. W. Rushforth, K. W. Edmonds, R. P. Campion, C. T. Foxon, B. L. Gallagher, and T. Jungwirth, Nat. Mater. **7**, 464 (2008).
[6] H. J. A. Molegraaf, J. Hoffman, C. A. F. Vaz, S. Gariglio, D. van der Marel, C. H. Ahn, and J. M. Triscone, Adv. Mater. (Weinheim, Ger.) **21**, 3470 (2009).
[7] T. Wu, S. B. Ogale, J. E. Garrison, B. Nagaraj, A. Biswas, Z. Chen, R. L. Greene, R. Ramesh, T. Venkatesan, and A. J. Millis, Phys. Rev. Lett. **86**, 5998 (2001).
[8] V. Garcia, M. Bibes, L. Bocher, S. Valencia, F. Kronast, A. Crassous, X. Moya, S. Enouz-Vedrenne, A. Gloter, D. Imhoff, C. Deranlot, N. D. Mathur, S. Fusil, K. Bouzehouane, and A. Barthelemy, Science **327** (5969), 1106 (2010).
[9] S. W. E. Riester, I. Stolichnov, H. J. Trodahl, N. Setter, A. W. Rushforth, K. W. Edmonds, R. P. Campion, C. T. Foxon, B. L. Gallagher, and T. Jungwirth, Appl. Phys. Lett. **94**, 063504 (2009).
[10] T. Jungwirth, K. Y. Wang, J. Masek, K. W. Edmonds, J. Konig, J. Sinova, M. Polini, N. A. Goncharuk, A. H. MacDonald, M. Sawicki, A. W. Rushforth, R. P. Campion, L. X. Zhao, C. T. Foxon, and B. L. Gallagher, Phys. Rev. B **72**, 165204 (2005).
[11] Y. Nishitani, D. Chiba, M. Endo, M. Sawicki, F. Matsukura, T. Dietl, and H. Ohno, Phys. Rev. B **81**, 045208 (2010).
[12] M. Sawicki, D. Chiba, A. Korbecka, Y. Nishitani, J. A. Majewski, F. Matsukura, T. Dietl, and H. Ohno, Nat. Phys. **6**, 22 (2010).
[13] K. Olejnik, M. H. S. Owen, V. Novak, J. Masek, A. C. Irvine, J. Wunderlich, and T. Jungwirth, Phys. Rev. B **78**, 054403 (2008).
[14] V. Novak, K. Olejnik, J. Wunderlich, M. Cukr, K. Vyborny, A. W. Rushforth, K. W. Edmonds, R. P. Campion, B. L. Gallagher, J. Sinova, and T. Jungwirth, Phys. Rev. Lett. **101**, 077201 (2008).
[15] A. Arrott, Phys. Rev. **108**, 1394 (1957).
[16] K. W. Edmonds, P. Boguslawski, K. Y. Wang, R. P. Campion, S. N. Novikov, N. R. S. Farley, B. L. Gallagher, C. T. Foxon, M. Sawicki, T. Dietl, M. Buongiorno Nardelli, and J. Bernholc, Phys. Rev. Lett. **92**, 037201 (2004).
[17] V. I. Litvinov and V. K. Dugaev, Phys. Rev. Lett. **86**, 5593 (2001).